



HAL
open science

**Transcriptional responses to exposure to the
brassicaceous defence metabolites camalexin and
allyl-isothiocyanate in the necrotrophic fungus
*Alternaria brassicicola***

Adnane Sellam, Anita Dongo, Piérick Hudhomme, Philippe Simoneau,
Thomas Guillemette

► **To cite this version:**

Adnane Sellam, Anita Dongo, Piérick Hudhomme, Philippe Simoneau, Thomas Guillemette. Transcriptional responses to exposure to the brassicaceous defence metabolites camalexin and allyl-isothiocyanate in the necrotrophic fungus *Alternaria brassicicola*. *Molecular Plant Pathology*, 2007, 8 (2), pp.195-208. 10.1111/j.1364-3703.2007.00387.x . hal-02665374

HAL Id: hal-02665374

<https://hal.inrae.fr/hal-02665374>

Submitted on 3 Mar 2023

HAL is a multi-disciplinary open access archive for the deposit and dissemination of scientific research documents, whether they are published or not. The documents may come from teaching and research institutions in France or abroad, or from public or private research centers.

L'archive ouverte pluridisciplinaire **HAL**, est destinée au dépôt et à la diffusion de documents scientifiques de niveau recherche, publiés ou non, émanant des établissements d'enseignement et de recherche français ou étrangers, des laboratoires publics ou privés.

Transcriptional responses to exposure to the brassicaceous defence metabolites camalexin and allyl-isothiocyanate in the necrotrophic fungus *Alternaria brassicicola*

ADNANE SELLAM^{1,†}, ANITA DONGO¹, THOMAS GUILLEMETTE¹, PIÉTRICK HUDHOMME² AND PHILIPPE SIMONEAU^{1*}

¹UMR PaVé No.77, Faculté des Sciences, 2 Bd Lavoisier, F-49045 Angers, France

²Chimie, Ingénierie Moléculaire et Matériaux d'Angers, UMR CNRS 6200 – Université d'Angers, 2 Bd Lavoisier, 49045 Angers, France

SUMMARY

Alternaria brassicicola is the causative agent of black spot disease of Brassicaceae belonging to the genera *Brassica* and *Raphanus*. During host infection, *A. brassicicola* is exposed to high levels of antimicrobial defence compounds such as indolic phytoalexins and glucosinolate breakdown products. To investigate the transcriptomic response of *A. brassicicola* when challenged with brassicaceous defence metabolites, suppression subtractive hybridization (SSH) was performed to generate two cDNA libraries from germinated conidia treated either with allyl isothiocyanate (AI-ITC) or with camalexin. Following exposure to AI-ITC, *A. brassicicola* displayed a response similar to that experienced during oxidative stress. Indeed, a substantial subset of differentially expressed genes was related to cell protection against oxidative damage. Treatment of *A. brassicicola* conidia with the phytoalexin camalexin appeared to activate a compensatory mechanism to preserve cell membrane integrity and, among the camalexin-elicited genes, several were involved in sterol and sphingolipid biosynthesis. The transcriptomic analysis suggested that protection against the two tested compounds also involved mechanisms aimed at limiting their intracellular accumulation, such as melanin biosynthesis (in the case of camalexin exposure only) and drug efflux. From the AI-ITC and the camalexin differentially expressed genes identified here, 25 were selected to perform time-course studies during interactions with brassicaceous hosts. *In planta*, up-regulation of all the selected genes was observed during infection of *Raphanus sativus* whereas only a subset were over-expressed during the incompatible interaction with *Arabidopsis thaliana* ecotype Columbia.

INTRODUCTION

Plants activate a variety of defensive mechanisms in response to challenges by fungal pathogens. Chemical defence mediated by host antimicrobial secondary metabolites has been demonstrated to be an efficient response to kill or inhibit the growth of invading fungi (Morrissey and Osbourn, 1999). These antimicrobial metabolites may be either constitutive compounds, also called phytoanticipins (Osbourn, 1996; Van Etten *et al.*, 1994), or biosynthesized *de novo* such as phytoalexins (Brooks and Watson, 1985). Both constitutive and induced chemical defences have been well documented in the plant model *Arabidopsis thaliana*. The indolic secondary metabolite camalexin is the major phytoalexin of this plant species. Mutation in the gene *PAD3*, encoding a cytochrome P450, abolishes the biosynthesis of camalexin (Glazebrook and Ausubel, 1994), and results in enhanced susceptibility to necrotrophic fungi (Thomma *et al.*, 1999). The phytoanticipins glucosinolates (GS) are sulphonated thioglycosides comprising a common glycone moiety with a variable aglycone side chain and are considered as the major secondary metabolites of Brassicaceae (Fahey *et al.*, 2001). Upon tissue damage, GS come into contact with myrosinases, a specific class of β -thioglucosidases, which are stored separately in the cell. Hydrolysis of GS by myrosinases yields isothiocyanates (ITC), nitriles and epithionitriles. The most common breakdown products, ITC, exhibit toxicity towards several plant pathogens including bacteria, fungi, insects and nematodes (Fahey *et al.*, 2001). It has been demonstrated that ITC produced by *Arabidopsis thaliana* significantly inhibit *in planta* growth of some fungal pathogens (Tierens *et al.*, 2001) although recent results suggest that apart from their direct toxic effects, GS breakdown products may also act by modulation of plant defence signalling (Brader *et al.*, 2006).

Alternaria brassicicola, a necrotrophic ascomycete, causes black spot disease on a wide range of Brassicaceae including weeds and crops. The cultivated plants *Brassica* and *Raphanus* spp. are susceptible to this disease, which is therefore economically important. During host infection, *A. brassicicola* is exposed

*Correspondence: Fax: +33 2 41 73 53 52; Tel: +33 2 41 73 54 53; E-mail: philippe.simoneau@univ-angers.fr

†Present address: Biotechnology Research Institute, National Research Council of Canada, 6100 Royalmount, Montreal, PQ, Canada.

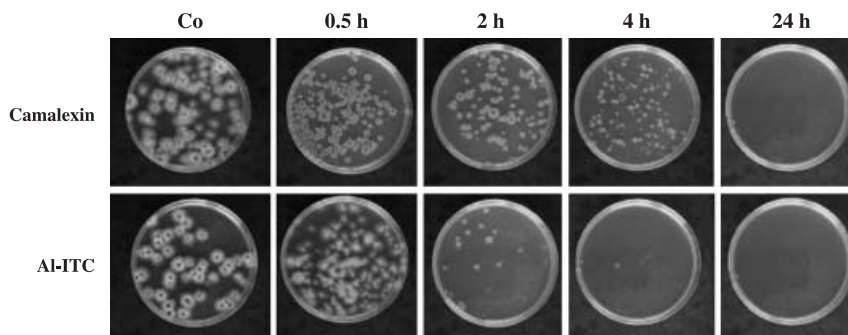


Fig. 1 Lethal effect of camalexin (125 μM) and AI-ITC (2.5 mM) on germinated *Alternaria brassicicola* conidia. The conidia ($2 \times 10^4 \text{ mL}^{-1}$) were germinated for 24 h in PDB, incubated for various times in the presence of the tested compound at the desired concentration and then applied on the Petri dishes containing PDA media. After 48 h of incubation colonies were visualized. Control plates (Co) were prepared with conidia incubated for up to 24 h with methanol or DMSO (1% v/v final concentration).

to high levels of phytoalexins and GS-breakdown products. Their ability to detoxify such chemical defence compounds may therefore constitute a key determinant of their virulence, as has been shown for several other fungi (Bowyer *et al.*, 1995; Quidde *et al.*, 1998). Cramer and Lawrence (2004) have shown that *CyHAB*, a cyanide hydratase-encoding gene, was up-regulated during the interaction of *A. brassicicola* with *Arabidopsis thaliana*, and suggested that this enzyme may be a candidate for the detoxification of GS-breakdown products. Recently, we have demonstrated that the ITC differentially expressed gene *AbGst1*, encoding a glutathione transferase, exhibiting high transferase activity with ITC as substrates, is also a candidate for ITC detoxification during host infection (Sellam *et al.*, 2006b).

To explore further *A. brassicicola* detoxification mechanisms against the major GS breakdown products ITC and brassicaceous phytoalexins, we have focused on the analysis of the transcriptional response in germinating conidia exposed either to the indolic phytoalexin camalexin produced by *Arabidopsis thaliana* and some brassicaceous weeds or to allyl-ITC (AI-ITC), a breakdown product of the aliphatic GS sinigrin produced by a variety of cruciferous vegetables. The identification of differentially expressed genes was performed with the suppression subtractive hybridization (SSH) technique and *in vitro* or *in planta* increased expression in response to plant compounds of several selected genes was confirmed by real-time quantitative PCR. The generated data provide insights on the cellular mechanisms by which the two studied compounds exert their toxicity and on the strategies used by the fungus to protect itself against these defence metabolites.

RESULTS AND DISCUSSION

Construction of the subtracted cDNA libraries

SSH was used to generate populations of cDNA corresponding to mRNA transcripts whose levels were increased after the exposure of *A. brassicicola* germinated conidia to sublethal concentrations of either the phytoalexin camalexin or the sinigrin breakdown product AI-ITC. To ensure that the observed changes in gene

expression not only reflected a non-specific response of the fungus to severe stress conditions, these treatments were performed using short periods of exposure (0.5 h) to concentrations of camalexin and AI-ITC that do not exceed the IC_{50} previously determined for this isolate by measuring their inhibitory effects on mycelial growth (Sellam *et al.*, 2006a). Under these conditions, cell viability did not differ from untreated controls, as revealed by plating assays (Fig. 1).

Subtraction efficiencies of the two cDNA libraries were very similar, as estimated using real-time PCR quantification of the housekeeping gene β -tubulin on the subtracted cDNA relative to the unsubtracted one. The cycle threshold (Ct) in the unsubtracted samples was obtained at ~ 15 cycles as opposed to ~ 27 cycles in the subtracted samples, thereby providing evidence for the efficiency and reproducibility of the SSH procedure. PCR analysis of 333 and 379 recombinant clones from the AI-ITC and camalexin libraries, respectively, revealed insert sizes ranging from ~ 200 to ~ 1500 bp (data not shown). Differential screening of the two libraries was performed using probes generated from the forward- and reverse-subtracted cDNA pools to select for positive clones, i.e. those exhibiting signal intensities more than five-fold higher with the forward-subtracted probes compared with the reverse-subtracted one. A total of 234 clones from the AI-ITC cDNA library and 280 clones from the camalexin cDNA library were thus selected for sequencing. After expressed sequence tag (EST) cluster analysis to remove sequence redundancies, a total of 76 and 112 unique ESTs were finally obtained for the AI-ITC and camalexin cDNA libraries, respectively.

Real-time quantitative PCR was performed to confirm further the differential expression of the identified sequences. From the AI-ITC cDNA library, a subset of 18 sequences was selected and their expressions were evaluated after exposure of conidia to AI-ITC and also to the aromatic ITC benzyl-ITC (Bz-ITC), a breakdown product of the GS glucotropaeolin (Table S1). As shown in Fig. 2, these experiments confirmed that the expression of all of the selected sequences was induced by AI-ITC following 0.5 h of exposure. After 2 h the expression of almost all the selected genes decreased back to the basal control levels, probably reflecting the strong inhibitory effect recorded for longer exposures to AI-ITC

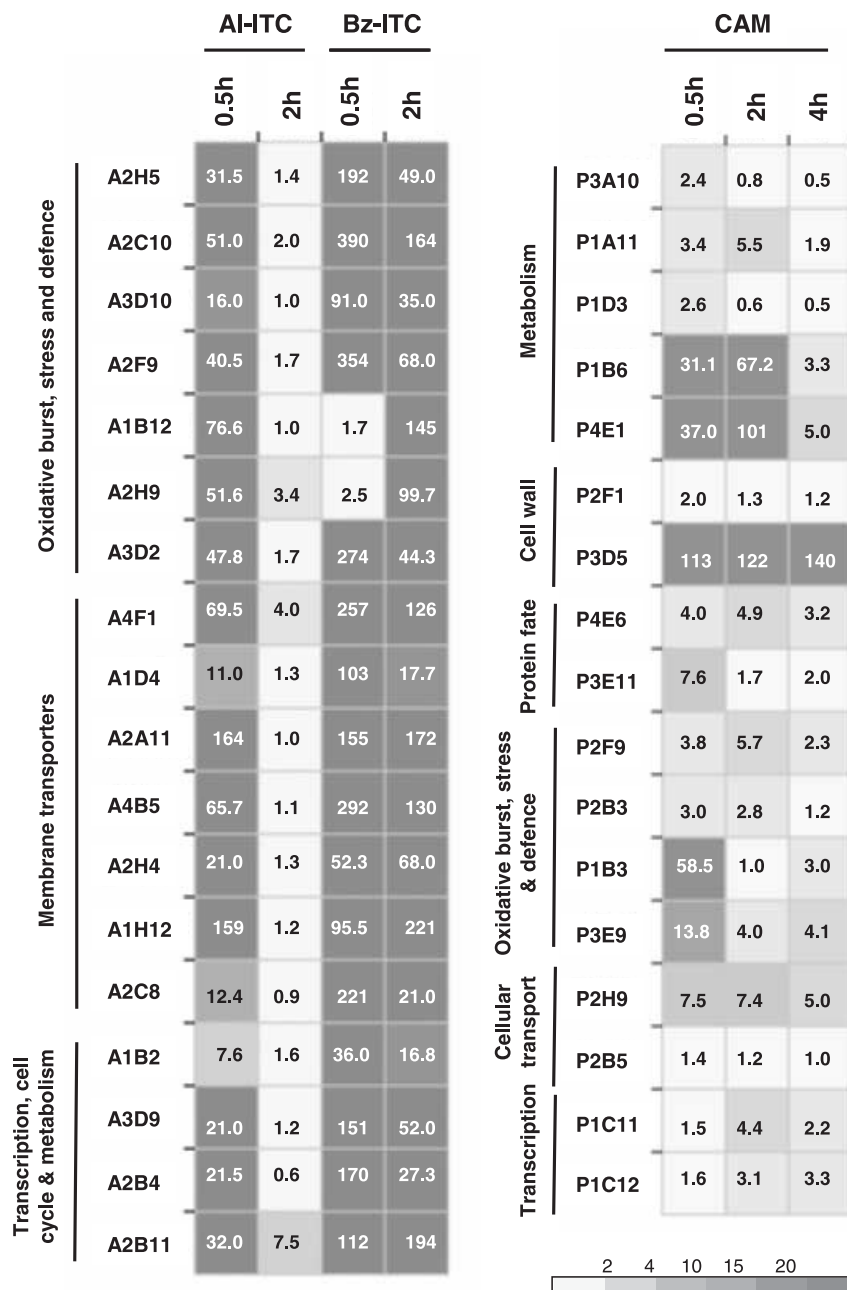


Fig. 2 Expression levels of sequences randomly selected from the AI-ITC (A) and camalexin (B) cDNA libraries in *Alternaria brassicicola* exposed to AI-ITC, Bz-ITC or camalexin. First-strand cDNAs were prepared from RNA samples extracted from germinated conidia exposed to AI-ITC (2.5 mM), Bz-ITC (0.3 mM) or camalexin (125 μM) for the indicated times and used as template for real-time PCR. For each gene, induction of expression is represented as a ratio (fold induction) of its relative expression (studied gene transcript abundance/ β -tubulin transcript abundance) in each inductive condition to its relative expression in the corresponding control (spores germinated in medium amended with the solvent only). Each value is the mean of two independent experiments each with three replicates. For easier visualization of the results, numerical data were transformed into colour-grid representations using the JColorGrid software (Joachimiak *et al.*, 2006) in which fold induction of gene expression is represented by a grey scale.

(see Fig. 1). Irrespective of the length of the treatment with Bz-ITC, all the selected genes were induced and their relative induction levels by this compound were higher compared with AI-ITC. It should be noted that, at the concentration used in this study (0.3 mM), no apparent loss of viability was observed after up to 2 h of exposure (data not shown). A total of 17 sequences were selected from the camalexin cDNA library and their differential expression levels were tested following exposure of conidia to camalexin for 0.5, 2 and 4 h (Table S2). The results of this assay revealed that transcript levels of most of the selected genes increased following exposure to camalexin (Fig. 2).

Functional classification of *A. brassicicola* genes expressed in response to ITC

To assign potential functions to the putative proteins encoded by SSH-generated cDNA fragments, the 76 AI-ITC unique EST sequences were analysed by comparing them to the GenBank non-redundant database sequences and the current complete genomes in the Fungal Genome Initiative project database using the BLASTX algorithm. Fifty-three sequences (71%) isolated from the AI-ITC cDNA library exhibited significant protein similarity to previously identified or putative proteins, and nine clones (11%)

Table 1 Summary of *Alternaria brassicicola* clones from the AI-ITC cDNA library. The presented ESTs correspond to those with significant matches (e-value < 1e-05) to proteins of known or predicted function.

Clone	GenBank accession no.*	Size†	Best BLAST match			e-value
			Accession no.	Organism	Annotation	
1. Oxidative burst, stress and defence						
A2H5	DY542653	724	CAC18210	<i>Neurospora crassa</i>	Putative microsomal glutathione S-transferase	6e-25
A1F1	DY542654	521	EAL87849	<i>Aspergillus fumigatus</i>	Putative glutathione S-transferase	1e-15
A2C1	DY542655	742	EAL87157	<i>A. fumigatus</i>	Putative glutathione S-transferase	4e-61
A2C10	DY542656	916	AAX07321	<i>A. fumigatus</i>	Similar to the glutathione S-transferase gstA	4e-48
A4D12	DY542657	886	BAB68404	<i>Gibberella fujikuroi</i>	Putative glutathione S-transferase	2e-39
A3D10	DY542658	808	O59858	<i>Schizosaccharomyces pombe</i>	Similar to the glutathione peroxidase gpx1	2e-49
A2F9	DY542659	713	CAA59379	<i>S. pombe</i>	Similar to the γ -glutamylcysteine synthetase Gcs1	1e-65
A3B11	DY542660	748	EAL92160	<i>A. fumigatus</i>	Putative γ -glutamylcysteine synthetase	8e-71
A3H11	DY542661	344	SNU08948.1	<i>Stagonospora nodorum</i>	Putative thioredoxin	4e-12
A2G8	DY542662	713	EAL89878	<i>A. fumigatus</i>	Putative thioredoxin	3e-23
A3G5	DY542663	555	EAL91252	<i>A. fumigatus</i>	Putative thioredoxin	1e-27
A1B12	DY542664	645	EAL88433	<i>A. fumigatus</i>	Putative DSBA-like thioredoxin	5e-22
A4D11	DY542665	711	P51978	<i>N. crassa</i>	Similar to the thioredoxin reductase cys9	1e-29
A3C8	DY542666	465	EAL87526	<i>A. fumigatus</i>	Putative NADH-dependent flavin oxidoreductase	2e-27
A2H9	DY542667	800	AAD41159	<i>S. pombe</i>	Similar to the sulphide-quinone oxidoreductase cad1	5e-46
A4B11	DY542668	948	SNU05420.1	<i>S. nodorum</i>	Putative Pyridine nucleotide-disulphide oxidoreductase	5e-07
A2B7	DY542669	326	SNU13823.1	<i>S. nodorum</i>	Putative Pyridine nucleotide-disulphide oxidoreductase	5e-08
A4A12	DY542670	735	BAC20562	<i>Penicillium citrinum</i>	Similar to the oxidoreductase mlcG	6e-18
A3A6	DY542671	700	CAF05989	<i>N. crassa</i>	Putative Hsc70-interacting protein	4e-16
A3G8	DY542672	600	S50131	<i>Aspergillus nidulans</i>	Similar to the heat-shock protein HSP30	6e-20
A4F3	DY542673	554	P19882	<i>Saccharomyces cerevisiae</i>	Similar to the heat-shock protein HSP60	4e-09
A3D2	DY542674	482	AAN74815	<i>G. moniliformis</i>	Similar to the Cytochrome P450 monooxygenase Fum12p	2e-37
2. Membrane transporters						
A4F1	DY542675	698	XP_365840	<i>M. grisea</i>	Putative ABC-type Fe ³⁺ transporter	2e-62
A1D4	DY542676	684	CAC41639	<i>Botryotinia fuckeliana</i>	Similar to the PDR ABC transporter BcAtrD	4e-29
A2A11	DY542677	486	CAA93140	<i>A. nidulans</i>	Similar to the PDR ABC transporter AtrA	3e-15
A4B5	DY542678	539	CAB46279	<i>Mycosphaerella graminicola</i>	Similar to the PDR ABC transporter MgAtr1	5e-42
A2H4	DY542679	462	Q06598	<i>S. cerevisiae</i>	Similar to the Arsenite transporter ACR3	2e-35
A1H12	DY542680	423	AAC44819	<i>Methanothermobacter thermautotrophicus</i>	Similar to the Formate/nitrite transporter FdhC	5e-20
A2C8	DY542681	710	AAC64976	<i>S. pombe</i>	Similar to the MFS hexose transporter ght6p	3e-64
A3H9	DY542682	373	XP_363585	<i>M. grisea</i>	Putative MFS transporter	1e-13
A4B2	DY542683	451	EAL92997	<i>A. fumigatus</i>	Putative MFS transporter	5e-14
A2A12	DY542684	492	EAL92132	<i>A. fumigatus</i>	Putative MFS transporter	4e-44
3. Transcription and cell cycle						
A4F6	DY542685	726	AAM08677	<i>A. fumigatus</i>	Similar to the Cell division control protein Cdc48p	2e-103
A1B2	DY542686	865	T37963	<i>S. pombe</i>	Similar to the caffeine-induced death protein Cid1	3e-14
A3D9	DY542687	614	O94684	<i>S. pombe</i>	Similar to the RNA polymerase II transcription factor pmh1	2e-35
A2B4	DY542688	1124	CAB98237	<i>N. crassa</i>	Similar to the positive-acting sulphur transcription factor CYS-3	1e-26
4. Metabolism						
A2B11	DY542689	1083	AAM88292	<i>Cochliobolus heterostrophus</i>	Similar to the Oxidoreductase RED1	6e-24
A4A8	DY542690	763	AAD09811	<i>A. nidulans</i>	Similar to the pantothenate kinase PanK	3e-57
A2A7	DY542691	423	CAA81612	<i>Geobacillus stearothermophilus</i>	Similar to the alcohol dehydrogenase ADH-HT	9e-12

*Twenty-three additional sequences that match to unclassified or hypothetical proteins have been registered under GenBank accession nos. DY542692 to DY542713. †In base pairs.

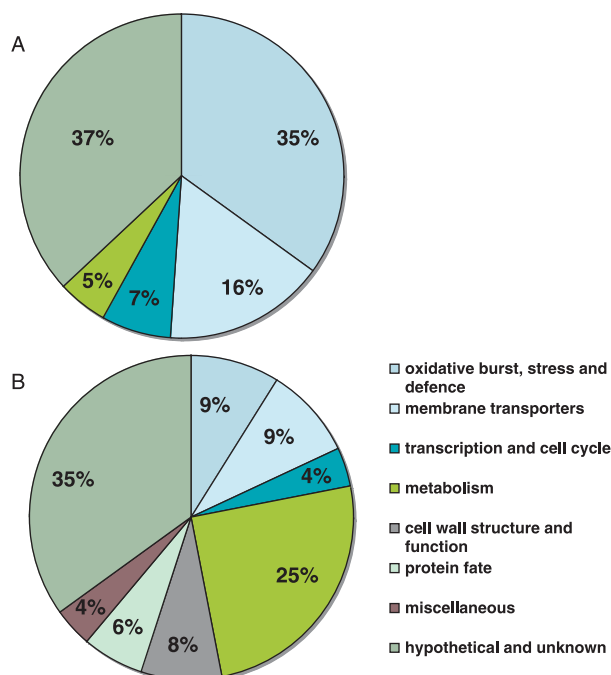


Fig. 3 Functional classification of up-regulated genes in *Alternaria brassicicola* AI-ITC- (A) and camalexin- (B) treated conidia according to their putative biological function.

contained inserts that showed similarity to conserved hypothetical proteins. No apparent similarity to known sequences was found for the inserts from the 14 remaining clones (18%). The set of sequences with significant matches to proteins of known or predicted function is listed in Table 1. These were assigned to four functional categories (Fig. 3A).

A significant portion of genes transcriptionally induced by AI-ITC such as glutathione transferases (GST), glutathione peroxidase, γ -glutamylcysteine synthetases, thioredoxins, thioredoxin reductase and oxidoreductases are involved in the oxidative stress response. The generation of reactive oxygen species (ROS) by ITC has already been reported in experimental animals (Nakamura *et al.*, 2000; Paolini *et al.*, 2004), resulting in the induction of the phase II enzymes NAD(P)H:Quinone oxidoreductase and GST activities and also the γ -glutamylcysteine synthetases catalysing the rate-limiting step in the formation of reduced glutathione (GSH) (McWalter *et al.*, 2004). Redox imbalance is probably caused by the depletion of the antioxidant GSH that reacts with ITC, resulting therefore in alterations of the oxidants/antioxidants ratio. An *A. brassicicola* cytochrome P450-encoding gene was induced by ITC. Interestingly, an EST corresponding to the same gene has already been detected in an *A. brassicicola*–*Brassica oleracea* SSH library and was shown to be induced *in planta* at 2 days post-infection (Cramer *et al.*, 2006). Similar phase I enzyme was also reported to be induced in animals by some dietary carcinogens including ITC (Paolini *et al.*, 2004). It therefore

appears that a redox imbalance occurs following the exposure of fungal cells to ITC, resulting in the activation of the conserved ITC-detoxification mechanism mediated by phase I and II enzymes. These results suggest, for the first time in fungi, that ITC causes oxidative stress, which is likely to be the origin of their cytotoxicity. Alternatively, ITC may induce antioxidant genes in *A. brassicicola* by direct activation of upstream signalling pathways without creating cellular oxidative stress. However, the results presented below (Fig. 4) showing the detection of intracellular reactive oxygen intermediates (ROI) after exposure of germinated conidia to ITC strongly support the first hypothesis.

Ten membrane transporters were induced by AI-ITC including four PDR-type ABC transporters and four MFS transporters. In fungi, ABC and MFS transporters represent different multidrug efflux pumps associated with resistance to xenobiotics and antibiotics including plant defence metabolites (Schoonbeek *et al.*, 2001; Urban *et al.*, 1999). The induction of these potential 'non-degradative' detoxification systems suggests that ITC is either removed directly from fungal cells or after being conjugated to GSH. In the yeast *Saccharomyces cerevisiae*, two ABC transporters have been shown to be GS-X pumps that catalyse the transport of glutathione conjugates into the vacuole (Li *et al.*, 1996; Sharma *et al.*, 2002). However, no apparent homology was found between the four isolated ITC-induced ABC transporters and the yeast GX pumps.

Interestingly, a gene encoding a positive-acting sulphur regulatory protein was identified from the AI-ITC cDNA library. In fungi, this transcription factor is required to turn on the expression of the sulphur-related metabolic enzymes (Natorff *et al.*, 2003). The transcriptional activation of this gene suggests that ITC, which are sulphur-containing metabolites, could be metabolized by *A. brassicicola* and used as a source of sulphur. Indeed, a stimulation of radial growth of *A. brassicicola* on solid medium containing low concentrations of AI-ITC or Bz-ITC was recorded compared with ITC-free medium (data not shown). Similarly, Giamoustaris and Mithen (1997) demonstrated that the level of *Alternaria* spp. infection was positively correlated with the GS content of leaves and pods of oilseed rape.

Functional classification of *A. brassicicola* genes expressed in response to camalexin

Details of the camalexin ESTs sequences that had significant matches to proteins of known or predicted function are given in Table 2. Among the 112 unique ESTs, 29 (25%) exhibited similarity to hypothetical proteins and 33 (30%) had no apparent similarity to known sequences. The remaining 50 ESTs (45%) that show homology to known or putative proteins were classified into six functional categories (Fig. 3B).

Genes responsive to camalexin included sphingolipid and ergosterol biosynthesis genes, which are essential compounds of

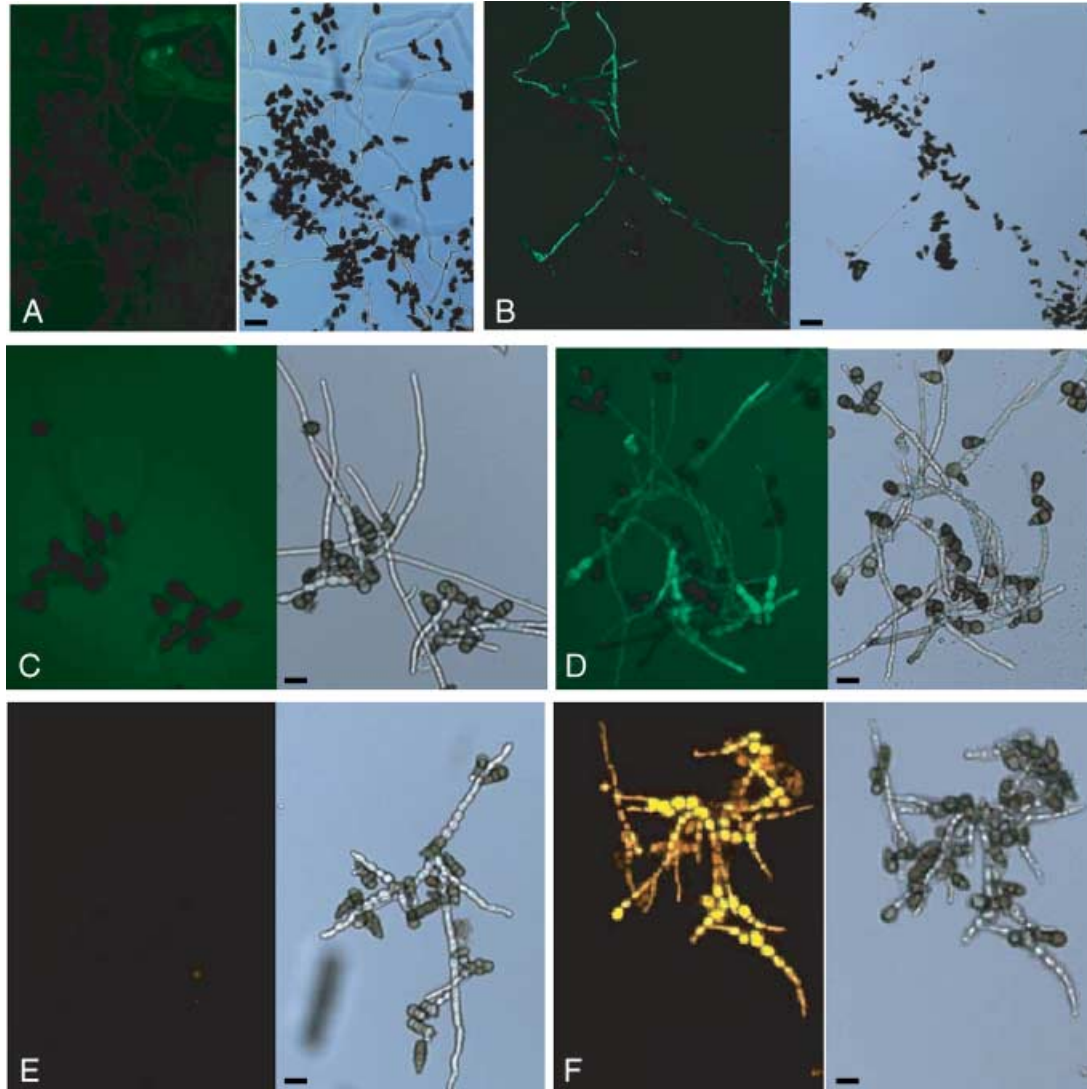


Fig. 4 Determination of membrane damage and oxidative stress symptoms in *Alternaria brassicicola* treated with camalexin and ITC. Membrane integrity was checked using SYTOX green uptake assays in 24-h germinated conidia treated for 24 h with DMSO 1% v/v (A) or 125 μ M camalexin (B). ROS within hyphae of germinated conidia treated for 4 h with methanol 1% v/v (C,E) or 2.5 mM AI-ITC (D,F) were detected using the fluorescent dyes H₂DCFDA (C,D) and DHE (E,F). For each panel, the left part corresponds to fluorescence microscopy and the right part to light-field microscopy. Scale bars = 20 μ m.

the fungal plasma membrane (Dickson and Lester, 2002; Parks and Casey, 1995). The induction of these genes in response to camalexin is somewhat similar to what was observed with *S. cerevisiae* and *Candida albicans* treated with azole fungicides, which are known to inhibit ergosterol biosynthesis (Bammert and Fostel, 2000; Liu *et al.*, 2005). Induction of the expression of the *A. brassicicola* *ERG3* gene encoding the sterol Δ 5,6-desaturase could be the consequence of ergosterol depletion, as demonstrated in the yeast *S. cerevisiae* after exposure to ergosterol biosynthesis-inhibitors (Liu *et al.*, 2005; Smith *et al.*, 1996). Several links between the biosynthetic pathway of ergosterol and other pathways involved in the biosynthesis of lipids have been already

highlighted in *S. cerevisiae* and *C. albicans* (Bammert and Fostel, 2000; Mukhopadhyay *et al.*, 2004; Veen and Lang, 2005) and these interactions probably constitute important determinants of drug susceptibility. By extrapolating to the present study, changes in the expression of these metabolic genes in response to camalexin are suggestive of alterations in the membrane integrity of the fungus. The damage caused by camalexin to the fungal cell surface may thus trigger a compensatory mechanism that would result in the activation of genes involved in membrane maintenance to ensure the stability of the cell. This would be consistent with the mechanism of action of camalexin on phytopathogenic bacteria reported by Rogers *et al.* (1996).

Table 2 Summary of *Alternaria brassicicola* clones identified from the camalexin cDNA library. The presented ESTs correspond to those with significant matches (e-value < 1e-05) to proteins of known or predicted function.

Clone	GenBank accession no.*	Size†	Best BLAST match			e-value
			Accession no.	Organism	Annotation	
1. Metabolism						
1.1. Lipid, fatty acid and sterol metabolism						
P3A10	DY543047	758	AAB41115	<i>S. cerevisiae</i>	Similar to the Sphinganine C4-hydroxylase Sur2p	4e-22
P1A11	DY543048	636	EAL87310	<i>A. fumigatus</i>	Putative delta 8-sphingolipid desaturase	2e-35
P2F2	DY543049	200	EAA74448	<i>G. zeae</i>	Putative sphingolipid hydroxylase	2e-05
P1H8	DY543050	1217	CAA84977	<i>S. cerevisiae</i>	Similar to the pyridoxine phosphate oxidase PDX3	2e-07
P1D3	DY543051	505	AAN27998	<i>Leptosphaeria maculans</i>	Similar to the sterol delta 5,6-desaturase ERG3	4e-42
1.2. Melanin biosynthesis						
P1B6	DY543052	788	BAA36503	<i>Alternaria alternata</i>	Similar to the 1,3,8-trihydroxynaphthalene reductase BRM2	9e-116
P4E1	DY543053	228	BAC79365	<i>Bipolaris oryzae</i>	Similar to the scytalone dehydratase BSCD1	2e-05
1.3. Other metabolism-linked genes						
P4E11	DY543054	1028	AA591580	<i>S. nodorum</i>	Putative glyoxysomal malate synthase	2e-69
P3A9	DY543055	595	P87208	<i>A. nidulans</i>	Similar to the pyruvate decarboxylase pdcA	5e-21
P3A3	DY543056	1112	SNU10756.1	<i>S. nodorum</i>	Putative zinc-binding dehydrogenase	2e-26
P1H4	DY543057	541	EAL86321	<i>A. fumigatus</i>	Putative D-xylulose 5-phosphate/b-fructose 6-phosphate phosphoketolase	3e-81
P4F3	DY543058	1161	AAN87355	<i>Paracoccidioides brasiliensis</i>	Putative formamidase	1e-23
P4C2	DY543059	620	EAL84490	<i>A. fumigatus</i>	Putative flavohemoprotein	2e-12
P2E7	DY543060	734	NP_014798	<i>S. cerevisiae</i>	Similar to the IMP-specific 5'-nucleotidase Isn1p	6e-45
P3D12	DY543061	625	EAL92794	<i>A. fumigatus</i>	Putative mitochondrial succinate dehydrogenase	4e-13
P4D8	DY543062	450	Q85HP8	<i>Hypocrea jecorina</i>	Similar to the NADH-ubiquinone oxidoreductase ND4L	1e-10
P2C2	DY543063	294	EAL91367	<i>A. fumigatus</i>	Putative oxidoreductase, 2OG-Fe (II) oxygenase family	4e-15
P3D8	DY543064	405	SNU13647.1	<i>S. nodorum</i>	Putative purine permease	3e-14
P3F12	DY543065	481	AAZ73168	<i>G. moniliformis</i>	Putative alpha-amylase 1	1e-06
P4D4	DY543066	645	CAA51009	<i>A. nidulans</i>	uricase	4e-28
2. Cell-wall structure and function						
P2F1	DY543067	460	AAC35942	<i>A. fumigatus</i>	Similar to the beta (1-3) glucanosyltransferases GEL1	2e-13
P4C8	DY543068	701	HJU89991	<i>H. jecorina</i>	Similar to the mannose-1-phosphate guanylyltransferase MPG1	7e-08
P3D5	DY543069	550	O74254	<i>C. albicans</i>	Putative cell wall mannoprotein glycosyl hydrolase	2e-19
P2B11	DY543070	367	EAL91687	<i>A. fumigatus</i>	Putative polysaccharide deacetylase	1e-54
P4A12	DY543071	561	EAL92848	<i>A. fumigatus</i>	Putative polysaccharide deacetylase	2e-11
P3C1	DY543072	1003	AA507042	<i>Chlamydomonas reinhardtii</i>	Similar to the minus agglutinin SAD1	5e-07
3. Protein fate						
P4A11	DY543073	732	CAA70219	<i>P. janthinellum</i>	Similar to the fructosyl amino acid oxidase FaoP	2e-30
P3F5	DY543074	489	YP_188090	<i>Staphylococcus epidermidis</i>	Putative cysteine desulphurase	2e-06
P4E6	DY543075	1118	Q9Y7P1	<i>S. pombe</i>	Similar to the endoplasmic oxidoreductin 1-like protein A ERO1p	2e-14
P3E11	DY543076	496	CAA07773	<i>G. pulicaris</i>	Similar to the polyubiquitin Ubi1	1e-38
P3H11	DY543077	450	SNU02705.1	<i>S. nodorum</i>	Putative proteasome non-ATPase regulatory subunit Nin1/mts3	3e-09
4. Oxidative burst, stress and defence						
P2F9	DY543078	400	EAL85706	<i>A. fumigatus</i>	Similar to the MFS drug transporter TRI12	9e-06
P2B3	DY543079	488	EAA75163	<i>G. zeae</i>	Putative MFS Transporter	2e-16
P1B3	DY543080	1108	AAC49410	<i>Nectria haematococca</i>	Similar to the flavin-containing mono-oxygenase MAK1	8e-17
P3E9	DY543081	578	ABC33908	<i>Tuber borchii</i>	Putative dehydrin	4e-09
P2D12	DY543082	626	P41747	<i>A. flavus</i>	Similar to the alcohol dehydrogenase adh1	1e-64
P2C10	DY543083	889	AAO73810	<i>P. brasiliensis</i>	Similar to the heat shock protein CLPA	1e-41
P2D5	DY543084	290	SNU00278.1	<i>S. nodorum</i>	Putative cation efflux transporter	1e-07
5. Cellular transport, transport facilitation and transport routes						
P2H9	DY543085	1031	AAN08046	<i>A. nidulans</i>	Similar to the siderophore iron transporter mirC	9e-55
P2B5	DY543086	829	P38865	<i>S. cerevisiae</i>	Similar to the copper transporter CTR2	8e-13

Table 2 *continued.*

Clone	GenBank accession no.*	Size†	Best BLAST match		Annotation	e-value
			Accession no.	Organism		
P3C4	DY543087	382	AAW42114	<i>Cryptococcus neoformans</i>	Putative cation transport-related protein	4e-06
P2C7	DY543088	483	ABB90287	<i>G. zeae</i>	Similar to the calcium-translocating P-type ATPase	1e-40
P3F9	DY543089	1089	EAL86522	<i>A. fumigatus</i>	Putative FAD dependent oxidoreductase	3e-46
P3E10	DY543090	530	SNU12213.1	<i>S. nodorum</i>	Putativethiamine pyrophosphate protein	1e-17
P2E6	DY543091	239	SNU15080.1	<i>S. nodorum</i>	Putative vacuolar protein sorting-associated protein 26	4e-11
6. Transcription						
P1C11	DY543092	818	EAL87704	<i>A. fumigatus</i>	Putative fungal specific transcription factor	3e-39
P1C12	DY543093	998	XP_893708	<i>Mus musculus</i>	Putative Histone H2A-Bbd	5e-11
P2B4	DY543094	464	O43003	<i>S. pombe</i>	Similar to the endoribonuclease L-PSP; translation initiation inhibitor Mmf1p	6e-15

*Thirty-one additional sequences that match to unclassified or hypothetical proteins have been registered under GenBank accession nos. DY543095 to DY543125. †In base pairs.

In addition to the ergosterol and sphingolipid biosynthesis genes, camalexin induced the expression of two melanin biosynthesis genes. An EST similar to the sequence from clone P1B6 encoding a 1,3,8-trihydroxynaphthalene reductase has already been derived from an *A. brassicicola*-*B. oleracea* SSH library and has been shown to be induced *in planta* as soon as 12 h after infection (Cramer *et al.*, 2006). The second EST (P4E1) from our camalexin SSH library is similar to the scytalone dehydratase, another key gene in the synthesis of melanin, which is a constitutive compound of the *Alternaria* conidia wall, located in the septa and outer primary wall (Carzaniga *et al.*, 2002). The induction of these genes occurred probably in an attempt to decrease cell-wall permeability and thus to prevent the intracellular accumulation of camalexin. The relationship between wall impermeability and protection against antifungal products has indeed already been demonstrated in *Cryptococcus neoformans* (Wang and Casadevall, 1994). Camalexin also induced the expression of several genes involved in cell-wall maintenance, including a gene encoding a $\beta(1-3)$ -glucanoyltransferase, which is homologous to the *Aspergillus fumigatus* *GEL1* gene involved in the elongation of β -1,3-glucan (Mouyna *et al.*, 2000), and the mannose-1-phosphate guanylyltransferase and mannoprotein glycosyl hydrolase genes implicated in cell-wall mannoprotein synthesis (Zakrzewska *et al.*, 2003; Zhao *et al.*, 2000). In addition to the induction of genes encoding proteins involved in melanin biosynthesis, changes in the expression of cell-wall biogenesis genes are also suggestive of a reinforcement of the physical barriers against the cellular penetration of toxic compounds.

As observed after AI-ITC challenge, exposure to camalexin resulted in enhanced expression of two efflux pumps belonging to the MFS superfamily that could actively participate to maintain low concentrations of this compound inside the fungal cell.

Interestingly, a gene encoding the flavin-containing monooxygenase homologous to the phytoalexin maackiain detoxifying enzyme *MAK1* was up-regulated by camalexin. In *Nectria haema-*

tococca the *MAK1* gene product converts a chick-pea phytoalexin maackiain into the less toxic compound 1a-hydroxy-maackiain (Covert *et al.*, 1996). Pedras and Khan (1997) reported that camalexin detoxification in *Rhizoctonia solani* may result from its conversion to the less toxic compound 5-hydroxycamalexin. It is therefore possible that camalexin hydroxylation could be also a potential detoxification mechanism in *A. brassicicola*.

Camalexin-induced membrane permeabilization

To check whether camalexin had an effect on fungal membrane integrity, an assay based on the uptake of the fluorogenic dye SYTOX green was used. This substance can only penetrate cells that have compromised plasma membranes, and it fluoresces upon binding to DNA. *A. brassicicola* germinated conidia were incubated with or without camalexin for various times and then the fluorescent probe was added. As shown in Fig. 4B, green fluorescence in hyphae was observed after treatment of germinated conidia exposed for 24 h with camalexin. Virtually no green fluorescence was detected in control samples treated with the fluorescent probes only (Fig. 4A). Samples incubated with camalexin for short time exposures, i.e. for times where the cell viability was not significantly affected by the treatment, did not significantly differ from controls (data not shown). These data indicated that camalexin probably causes membrane damage.

ITC-induced production of cellular reactive oxygen intermediates

To obtain additional support for the generation of an oxidative stress by ITC in fungal cells, the production of ROI was assessed using 2',7'-dichlorodihydrofluorescein diacetate (H₂DCF-DA), which is hydrolysed within the cells to 2',7'-dichlorodihydrofluorescein (H₂DCF), which reacts with peroxides to generate the fluorescent

compound 2',7'-dichlorofluorescein (DCF). After 4 h of incubation with either AI- or Bz-ITC (Fig. 4D), DCF-dependent fluorescence was observed in hyphae whereas no signal was recorded in untreated controls (Fig. 4C). To confirm these data further, dihydroethidium (DHE), a redox-sensitive probe that is oxidized to ethidium by superoxide anions, was also used to detect intracellular ROI after exposure to ITC. Fluorescence intensity of hyphae was strongly increased in samples exposed for 4 h to either AI- or Bz-ITC (Fig. 4F) compared with untreated controls (Fig. 4E). These observations confirmed that ITC are potential inducers of intracellular ROI in fungal cells, as was shown for animal cells (Nakamura *et al.*, 2000).

Expression of candidate genes during *Arabidopsis thaliana* and *Raphanus sativus* infection

In order to address the question of expression of the plant-compound-responsive genes in compatible vs. incompatible interactions, 25 candidate genes were selected from the two cDNA libraries on the basis of their similarity to known proteins potentially involved in cell protection, detoxification and transcription regulation. Expression time-course studies during *A. brassicicola* interaction with the resistant weed *Arabidopsis thaliana* and also with the susceptible host *R. sativus* were then performed.

Results of the time-course experiment during interaction with *Arabidopsis thaliana* (Fig. 5A; Table S3) revealed that among the ITC-up-regulated candidate genes, the expression levels of all transporters were induced as well as the thioredoxin and the sulphide-quinone oxidoreductase encoding cDNA. *In planta* increased expression levels of camalexin-induced genes were recorded for the sequences P1C11, P1C12, P2F9 and P4E1 encoding homologues of MFS transporter, histone H2A-binding, fungal-specific transcription factor and scytalone dehydratase, respectively. During interaction with the host *R. sativus*, the expression of all the candidate genes was significantly induced, except for the camalexin-induced sequence P2H9 encoding a putative siderophore transporter (Table S4).

Fungal biomass evolution during the interaction with both *Arabidopsis thaliana* (Fig. 5B) and *R. sativus* (Fig. 5C) was also followed by measuring the amount of *A. brassicicola* DNA in plant tissues. Fungal biomass remained stable during the incompatible interaction with *Arabidopsis thaliana* Co, which is consistent with the fact that this accession is resistant to this fungus. During infection of the compatible host *R. sativus*, *A. brassicicola* biomass increased significantly during the time-course of the experiment, indicating an invasive growth of the fungus in this susceptible plant.

These results demonstrated that almost all the selected ITC and camalexin candidate genes were up-regulated during the compatible interaction with *R. sativus*, whereas only a few genes were induced during the incompatible interaction with *Arabidopsis*

thaliana. However, a possible transient expression, not covered by our time-course experiment, cannot be ruled out. It should be noted that the selected camalexin-induced genes were up-regulated during interaction with *R. sativus* while this plant is not known to produce this phytoalexin. This suggests that these genes may also be activated in response to other derivatives of this indolic phytoalexin, such as 6-methoxycamalexin, which is produced by *R. sativus* (Pedras *et al.*, 2000).

CONCLUSION

The present study reports the results of an analysis of the responses of *A. brassicicola* to short time exposures to brassicaceous metabolites at concentrations that are likely to be found in plant tissues during infection in the area surrounding necrotic lesions (Kliebenstein *et al.*, 2005). Two distinct gene induction profiles were obtained for the two tested compounds, implying that the recorded responses were not simply a general response of the fungus to severe stress conditions. This was further supported by the *in planta* induction of almost all the selected candidate genes during the compatible interaction with *R. sativus*. The data generated using both SSH and cellular fluorescent probes suggest possible mechanisms of cytotoxicity for ITC and camalexin on the fungus and shed light on the differences in cellular responses to these two different defence compounds. In the presence of ITC, fungal cells displayed responses similar to those experienced during oxidative stress, while camalexin activated the so-called 'compensatory mechanism' aimed at preserving membrane integrity. Furthermore, the expression of some efflux pumps was remarkably increased in response to ITC and camalexin, suggesting that efflux mechanisms could also be a potential detoxification pathway in *A. brassicicola*. Some of the genes identified here, by allowing the fungus to overcome the toxic effects of plant defence compounds, should be added to the growing list of potential *A. brassicicola* virulence factors together with the recently published expressed sequence tags derived from an *A. brassicicola*—*B. oleracea* interaction (Cramer *et al.*, 2006). Thanks to the forthcoming *A. brassicicola* genome annotation and the recent development of an efficient method for gene disruption in this fungus (Cho *et al.*, 2006), functional analyses of several of these candidate genes may soon be performed.

EXPERIMENTAL PROCEDURES

Antimicrobial metabolites

AI-ITC and Bz-ITC were purchased from Aldrich Chemical Co. (Milwaukee, WI). The phytoalexin camalexin was synthesized according to Ayer *et al.* (1992). Stock solutions (100-fold concentrated) were prepared using methanol and dimethyl sulphoxide (DMSO) as solvents for ITC and camalexin, respectively.

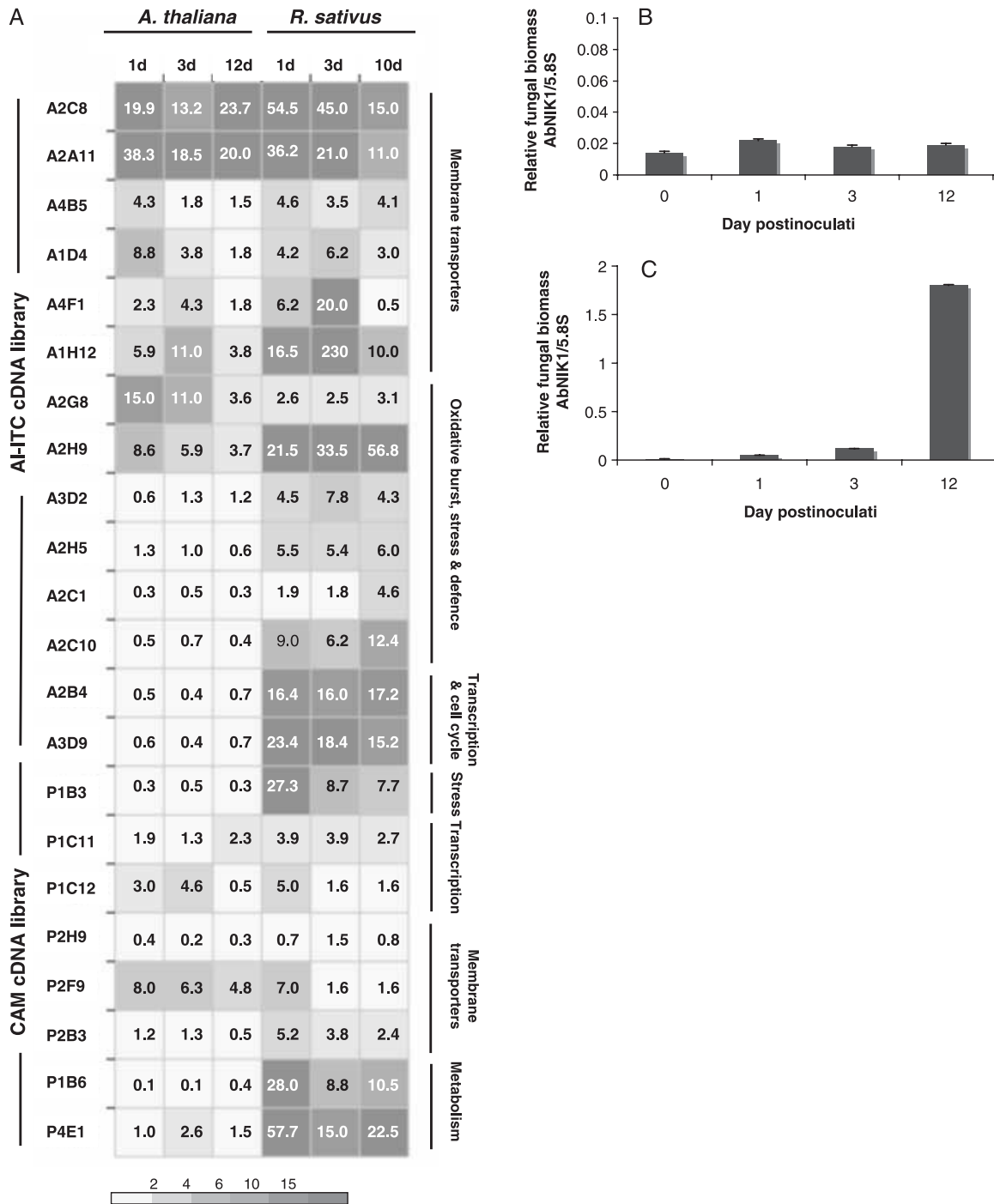


Fig. 5 Expression levels of sequences selected from the AH-TC and camalexin cDNA libraries during the interaction between *Alternaria brassicicola* and *Arabidopsis thaliana* or *Raphanus sativus*. (A) First-strand cDNAs were prepared from RNA samples extracted from plant tissues at the indicated times after inoculation and used as template for real-time PCR. For each gene, induction of expression is represented as a ratio (fold induction) of its relative expression (studied gene transcript abundance/ β -tubulin transcript abundance) in each inoculated sample to its relative expression in free-living fungal control cultures. Each value is the mean of two independent experiments each with three replicates. For easier visualization of the results, numerical data were transformed into colour-grid representations using the JColorGrid software (Joachimiak *et al.*, 2006) in which fold induction of gene expression is represented by a grey scale. (B,C) Fungal growth quantification during interaction with *Arabidopsis thaliana* and *R. sativus*, respectively. The abundance of *AbNIK1* was quantified in infected leaves, normalized with plant 5.8S ribosomal DNA and expressed by the ratio of the fungal *AbNIK1* DNA amount to plant 5.8S ribosomal DNA (*AbNIK1*/5.8S). The data are the mean of three repetitions. The star indicates the beginning of conidia germination and leaf tissue penetration.

Fungal strain, growth conditions, plant infection and pathogenicity assay

The *A. brassicicola* wild-type strain Abra43 used in this study was isolated from *R. sativus* seeds. Its taxonomic status has already been confirmed, using both morphological and molecular criteria (Iacomi-Vasilescu *et al.*, 2002). For routine culture, *A. brassicicola* was grown and maintained on potato dextrose agar (PDA). Antimicrobial compounds were added at concentrations equivalent to or below the IC₅₀ for mycelial growth (2.5 mM AI-ITC, 300 µM Bz-ITC, 125 µM camalexin), to 2-day-old germinating conidia grown in potato dextrose broth (PDB). Incubation in the presence of the fungus was then carried out for 0.5, 2, 4 and 24 h. Controls were performed by adding the relevant solvent (1% v/v final concentration) instead of the tested compound. Assays for viability were performed at each time point by spreading aliquots of treated or control conidia suspension on to PDA plates. Mycelial colonies developed after 48 h of incubation were scored. All culturing was performed at 24 °C.

Arabidopsis thaliana Co plants were grown to the eight- to 12-leaf stage in controlled environment rooms (21/19 °C day/night temperature, respectively) and an 8-h light photoperiod. For inoculations, 5-µL drops of a freshly prepared *A. brassicicola* spore suspension (5 × 10⁶ spores/mL in water) were pipetted on to six leaves per plant (two drops per leaf). The plants were then maintained under saturating humidity (100% relative humidity). Control plants were not inoculated, but were otherwise treated in the same way.

To assess fungal development and disease severity during the interaction, fungal DNA was quantified by real-time quantitative PCR as described by Sellam *et al.* (2006b) using the *A. brassicicola* histidine kinase *AbNIK1* gene (AY700092) as target sequence.

Suppression-subtractive hybridization

SSH cDNA was synthesized from 1 µg total RNA, isolated from *A. brassicicola* as previously described (Guillemette *et al.*, 2004), using the Super SMART PCR cDNA synthesis kit (Clontech, Palo Alto, CA) as described in the user manual. The cDNA populations were then subtracted using the PCR-Select cDNA subtraction kit (Clontech) following the manufacturer's instructions. The PCR products derived from the final SSH step were ligated into the pGEM-T vector (Promega, Charbonnières, France) and transferred into *Escherichia coli* JM109 cells to generate libraries of SSH-derived fragments.

Differential screening of the subtracted library by reverse dot-blot

cDNA inserts of putative recombinant clones were amplified from 1 µL of an overnight culture using nested primers and PCR conditions as described in the manual of the PCR-Select cDNA subtraction kit. After amplification, the PCR products were analysed

by gel electrophoresis to confirm the presence of an insert in each recombinant clone. Two microlitres of the denatured PCR products were blotted on to duplicate Hybond-N+ nylon membranes (Amersham, Buckinghamshire, UK) using a Minifold® dot-blotter (Schleicher & Schuell BioScience, Dassel, Germany). Forward and reverse subtracted probes were labelled with ³²P using a random primer labelling kit (Amersham). The labelled cDNA probes were hybridized to the dot-blot membranes at 72 °C overnight with continuous agitation. After hybridization, membranes were washed with low-stringency (2× SSC and 0.5% SDS) solution at 68 °C followed by high-stringency (0.2× SSC and 0.5% SDS) solution at the same temperature for 30 min each. The wet membranes were then exposed to Kodak K-screens and blots were visualized on a phosphorimager (Molecular Imager FX, Bio-Rad, Hercules, CA) and analysed using Quantity one software (Bio-Rad).

Clone sequencing and analysis

The selected positive clones were all sequenced with T7 primer by the automated sequencing facility of Ouest-Génopole (Roscoff, France) using the AB3130 genetic analyser (Applied Biosystems, Foster City, CA). Unique ESTs were selected and annotated on the basis of the existing annotation of non-redundant GenBank database sequences using the BLASTX algorithm. Functional classification was carried out according to the functional categories of the yeast *S. cerevisiae* proteins (<http://www.yeastgenome.org/>). EST sequences have been submitted to the GenBank EST database under the accession numbers given in Tables 1 and 2.

Expression analysis by real-time quantitative PCR

Traces of genomic DNA contaminants were removed by treating total RNA with TURBO™ DNase (Ambion, Huntingdon, UK). The absence of contaminating genomic DNA in the RNA samples was determined by direct amplification of non-reverse transcribed samples. cDNA was synthesized from 5 µg of total RNA using the reverse-transcription system (50 mM Tris-HCl, 75 mM KCl, 10 mM dithiothreitol, 3 mM MgCl₂, 400 nM oligo(dT)15, 1 µM random hexamers, 0.5 mM dNTP, 200 units M-MLV reverse transcriptase; Promega). The total volume was adjusted to 30 µL and the mixture was then incubated for 60 min at 42 °C. Aliquots of the resulting first-strand cDNA were used for real-time PCR amplification experiments. Real-time PCRs were performed with the ABI Prism 7000 sequence detection system (Applied Biosystems) using the SYBR green PCR master mix, according to the manufacturer's instructions. After 10 min denaturation at 95 °C, the reactions were cycled 40 times at 95 °C for 15 s and 60 °C for 1 min. To verify that only the specific product was amplified, a melting point analysis was performed after the last cycle by cooling samples to 55 °C and then increasing the temperature to 95 °C at 0.2 °C/s. A single product at a specific melting temperature was found for

Gene	5' primer	3' primer
β -Tubulin	TCAACGAAGCTCCAACAAC	GTGCCGGGCTCGAGAT
A2H5	GTACCCATACGAATACGCATCCTA	GCATTCGCGCTCTGGATT
A2C10	GCCAACCACTTCAACCGTTT	TCGCCTGTATAACGCTGCAT
A3D10	GGCTCCCCTACGATCTCA	TTCGAGGCGGTGTGACA
A2F9	CCGACATCAAGCAGCGTCTA	AGCAAAATGGGTCGCTAGGA
A1B12	GAAAAGAGCGCACAGCAATG	AAAATTGATCCCCTCGTCTTGTG
A2H9	CGACAACCTGCTTGACGCTACA	GATGCCTGGCGCAATGAC
A3D2	GCGGCTTGATCAAGGAA	GGCGCGGAAGTCCAAGT
A4F1	TCCAGACGCTGCACGAGTT	AACGGCGGTAGTTCATCA
A1D4	CTTGACAGCGCCCTTGTTG	GCCCAAGCCAAAAGGA
A2A11	GAGAAGGGTGCACAACAAG	GGTGCCAGCATCCTTCTCA
A4B5	ACATCAAAGCCAGCGACAAGT	CCCAATTGCTGACGCAGAA
A2H4	CCAGGCCACCAAAATCAG	TTGCATGGGCGTCTTACC
A1H12	CACCTTTCGCGCTCTCTTC	CCACAGCCCAGACAATTTGGT
A2C8	CGCCCGTGGTATCTTGTC	TCGGCTGTGATCTTGGTGTG
A1B2	CGCCCGTGGTATCTTGTC	TCGGCTGTGATCTTGGTGTG
A3D9	TCGTGATCCGTGGACTCAA	CGGGTCGAAGGGTGTCT
A2B4	CTCCGTCTGCACTGCTGTATC	AGTCCCAGAAGGAGGCACAA
A2B11	GCGCTAATATGCTATGCTTTGC	ACGGAATCTACCCGGGAATATACT
P3A10	CGGGCTTGCTGTGAGA	CAACGATGATCTTCTAACCACAA
P1A11	GCGCTCATGAACCGCTATC	GGCGGTAGGAAGTGTATCCA
P1D3	TCGCGATACGTCGTGTGTT	TCCATCCCATCACCAGTCTTT
P1B6	GACGACGTTGTGCCATT	AGAAACGACACCGGAGTTTGA
P4E1	GGCGCCGTAGGAAATGTG	CCCCATCATCTCGTATTGC
P2F1	CCCCGGGCTGGTAGTC	CCGTACCGGTCAAAGGAAA
P3D5	GCGCTTGCAACGTGACTAT	TTGTCTCCCCATCAACTTAACC
P4E6	ATTTCGAAGCCGCAAAAAG	CAAGCCCCCAAGGAAAG
P3E11	GCAGGGCAAATCATCTATGA	GTCCCTGATGGTCGATGAC
P2F9	GGTCTGCGCCGTGATTA	CCAATTAGCCACCCGATTT
P2B3	TCGACCTCGCTTATCAAAGG	GCGTAGCATATCCAAGCAAACC
P1B3	CGTACGAGGCAGATGTAGTCA	CAACAAGCTCCGGCTCTTC
P3E9	CGTGGACCATCGTCTGAT	GCATCGTCTATCTACGTGTCTGGTA
P2H9	CCGGCAGAATAACAGCTCAGA	GCAGGCGATTACACCAACA
P2B5	TCAGCCAGTCTTCGTCAACAA	CGCGCCAGCTGTCTAACTTT
P1C11	GCTTTCCATCACACCATGTGT	CTTGACGGGCGCATTGA
P1C12	GGTGCCGTATGAGTGGAGCTA	CGTGGAAAGAGCGCAGTGA

Table 3 Primer sets used in real-time quantitative PCR.

each target. All samples were tested in triplicate and the mean was determined for further calculations. Each run included a no-template control to rule out test reagent contamination.

The relative quantification analysis was performed using the comparative $\Delta\Delta C_t$ method as described by Winer *et al.* (1999). To evaluate the gene expression level, the results were normalized using C_t values obtained from β -tubulin RNA amplifications run on the same plate. Primer sequences used in real-time quantitative PCR are summarized in Table 3.

SYTOX green uptake assay and intracellular detection of oxidative products

For membrane permeabilization assays, 2-day-old germinating conidia were exposed to either 125 μ M camalexin or 1% (v/v)

DMSO as negative control as described for viability tests, for the indicated times. After treatment, 20 μ L of incubation mixtures were mixed with a SYTOX green solution (1 μ M final concentration) and immediately observed with a Zeiss fluorescence microscope. Essentially the same procedure was used to detect intracellular ROI after exposure to 2.5 mM Al-ITC or 0.3 mM Bz-ITC or 1% (v/v) methanol. After treatment, 100 μ L of incubation mixtures were mixed with H₂DCF-DA or DHE solutions (5 μ M final concentration) and observations were performed as above after 30 min of incubation.

ACKNOWLEDGEMENTS

This work was supported by the 'Contrat de Plan Etat-Région Pays de Loire' (2000–2006). We wish to thank the 'Conseil Général de Maine et Loire' for providing A.S. with a PhD fellowship. We thank

Dr Andrew Plumridge and Dr Kerry Ferguson for correcting the English version of the manuscript.

REFERENCES

- Ayer, W.A., Craw, P.A., Ma, Y. and Miao, S. (1992) Synthesis of camalexin and related phytoalexins. *Tetrahedron*, **48**, 2919–2924.
- Bammert, G.F. and Fostel, J.M. (2000) Genome-wide expression patterns in *Saccharomyces cerevisiae*: comparison of drug treatments and genetic alterations affecting biosynthesis of ergosterol. *Antimicrob. Agents Chemother.* **44**, 1255–1265.
- Bowyer, P., Clarke, B., Lunness, P., Daniels, M. and Osbourn, A. (1995) Host range of a plant pathogenic fungus determined by a saponin detoxifying enzyme. *Science*, **20**, 267371–267374.
- Brader, G., Mikkelsen, M.D., Halkier, B.A. and Palva, E.T. (2006) Altering glucosinolate profiles modulates disease resistance in plants. *Plant J.* **46**, 758–767.
- Brooks, C.J.W. and Watson, D.G. (1985) Phytoalexins. *Nat. Prod. Report*, **2**, 427–459.
- Carzaniga, R., Fiocco, D., Bowyer, P. and O'Connell, R.J. (2002) Localization of melanin in conidia of *Alternaria alternata* using phage display antibodies. *Mol. Plant–Microbe Interact.* **15**, 216–224.
- Cho, Y., Davis, J.W., Kin, K.H., Wang, J., Sun, Q.H., Cramer, R.A. and Lawrence, C.B. (2006) A high throughput targeted gene disruption method for *Alternaria brassicicola* functional genomics using linear minimal element (LME) constructs. *Mol. Plant–Microbe Interact.* **19**, 7–15.
- Covert, S.F., Enkerli, J., Miao, V.P. and VanEtten, H.D. (1996) A gene for maackiain detoxification from a dispensable chromosome of *Nectria haematococca*. *Mol. Gen. Genet.* **251**, 397–406.
- Cramer, R.A., La Rota, C.M., Cho, Y., Thon, M., Craven, K.D., Knudson, D.L., Mitchell, T.K. and Lawrence, C.B. (2006) Bioinformatic analysis of expressed sequence tags derived from a compatible *Alternaria brassicicola*–*Brassica oleracea* interaction. *Mol. Plant Pathol.* **7**, 113–124.
- Cramer, R.A. and Lawrence, C. (2004) Identification of *Alternaria brassicicola* genes expressed *in planta* during pathogenesis of *Arabidopsis thaliana*. *Fungal. Genet. Biol.* **41**, 115–128.
- Dickson, R.C. and Lester, R.L. (2002) Sphingolipid functions in *Saccharomyces cerevisiae*. *Biochim. Biophys. Acta*, **1583**, 13–25.
- Fahey, J.W., Zalemann, A.T. and Talahay, P. (2001) The chemical diversity and distribution of glucosinolates and isothiocyanates among plants. *Phytochemistry*, **56**, 5–51.
- Giamoustaris, A. and Mithen, R. (1997) Glucosinolates and disease resistance in oilseed rape (*Brassica napus* ssp. *oleifera*). *Plant Pathol.* **46**, 271–275.
- Glazebrook, J. and Ausubel, F.M. (1994) Isolation of phytoalexin-deficient mutants of *Arabidopsis thaliana* and characterization of their interactions with bacterial pathogens. *Proc. Natl Acad. Sci. USA*, **91**, 8955–8959.
- Guillemette, T., Sellam, A. and Simoneau, P. (2004) Analysis of a nonribosomal peptide synthetase gene from *Alternaria brassicae* and flanking genomic sequences. *Curr. Genet.* **45**, 214–224.
- Iacomi-Vasilescu, B., Blanchard, D., Guénard, M., Molinero-Demilly, V., Laurent, E. and Simoneau, P. (2002) Development of a PCR based diagnostic assay for detecting pathogenic *Alternaria* species in cruciferous seeds. *Seed. Sci. Technol.* **30**, 87–95.
- Joachimiak, M.P., Weisman, J.L. and May, B.C.H. (2006) JColorGrid: software for the visualization of biological measurements. *BMC Bioinfo.* **7**, 225–229.
- Kliebenstein, D.J., Rowe, H.C. and Denby, K.J. (2005) Secondary metabolites influence *Arabidopsis/Botrytis* interactions: variation in host production and pathogen sensitivity. *Plant J.* **44**, 25–36.
- Li, Z.S., Szczypka, M., Lu, Y.P., Thiele, D.J. and Rea, P.A. (1996) The yeast cadmium factor protein (YCF1) is a vacuolar glutathione S-conjugate pump. *J. Biol. Chem.* **271**, 6509–6517.
- Liu, T.T., Lee, R.E., Barker, K.S., Lee, R.E., Wei, L., Homayouni, R. and Rogers, P.D. (2005) Genome-wide expression profiling of the response to azole, polyene, echinocandin, and pyrimidine antifungal agents in *Candida albicans*. *Antimicrob. Agents Chemother.* **49**, 2226–2236.
- McWalter, G.K., Higgins, L.G., McLellan, L.I., Henderson, C.J., Song, L., Thornalley, P.J., Itoh, K., Yamamoto, M. and Hayes, J.D. (2004) Transcription factor Nrf2 is essential for induction of NAD(P)H:quinone oxidoreductase 1, glutathione S-transferases, and glutamate cysteine ligase by broccoli seeds and isothiocyanates. *J. Nutr.* **134**, 3499S–3506S.
- Morrissey, J.P. and Osbourn, A.E. (1999) Fungal resistance to plant anti-biotics as a mechanism of pathogenesis. *Microbiol. Mol. Biol. Rev.* **63**, 708–724.
- Mouyna, I., Fontaine, T., Vai, M., Monod, M., Fonzi, W.A., Diaquin, M., Popolo, L., Hartland, R.P. and Latge, J.P. (2000) Glycosylphosphatidylinositol-anchored glucanase transferases play an active role in the biosynthesis of the fungal cell wall. *J. Biol. Chem.* **275**, 14882–14889.
- Mukhopadhyay, K., Prasad, T., Saini, P., Pucadyil, T.J., Chattopadhyay, A. and Prasad, R. (2004) Membrane sphingolipid–ergosterol interactions are important determinants of multidrug resistance in *Candida albicans*. *Antimicrob. Agents Chemother.* **48**, 1778–1787.
- Nakamura, Y., Ohigashi, H., Masuda, S., Murakami, A., Morimitsu, Y., Kawamoto, Y., Osawa, T., Imagawa, M. and Uchida, K. (2000) Redox regulation of glutathione S-transferase induction by benzyl isothiocyanate: correlation of enzyme induction with the formation of reactive oxygen intermediates. *Cancer Res.* **60**, 219–225.
- Natorff, R., Sienko, M., Brzywczy, J. and Paszewski, A. (2003) The *Aspergillus nidulans* *metR* gene encodes a bZIP protein which activates transcription of sulphur metabolism genes. *Mol. Microbiol.* **49**, 1081–1094.
- Osbourn, A.E. (1996) Preformed antimicrobial compounds and plant defence against fungal attack. *Plant Cell*, **8**, 1821–1831.
- Paolini, M., Perocco, P., Canistro, D., Valgimigli, L., Pedulli, G.F., Iori, R., Croce, C.D., Cantelli-Forti, G., Legator, M.S. and Abdel-Rahman, S.Z. (2004) Induction of cytochrome P450, generation of oxidative stress and *in vitro* cell-transforming and DNA-damaging activities by glucoraphanin, the bioprecursor of the chemopreventive agent sulforaphane found in broccoli. *Carcinogenesis*, **25**, 61–67.
- Parks, L.W. and Casey, W.M. (1995) Physiological implications of sterol biosynthesis in yeast. *Annu. Rev. Microbiol.* **49**, 95–116.
- Pedras, M.S.C. and Khan, A.Q. (1997) Unprecedented detoxification of the cruciferous phytoalexin camalexin by a root phytopathogen. *Bioorg. Med. Chem. Lett.* **7**, 2255–2260.
- Pedras, M.S.C., Okanga, F.I., Zaharia, I.L. and Khan, A.Q. (2000) Phytoalexins from crucifers: synthesis, biosynthesis and biotransformation. *Phytochemistry*, **53**, 161–176.
- Quidde, T., Osbourn, A. and Tudzynski, P. (1998) Detoxification of alpha-tomatine by *Botrytis cinerea*. *Physiol. Mol. Plant Pathol.* **52**, 151–165.
- Rogers, E.E., Glazebrook, J. and Ausubel, F.M. (1996) Mode of action of the *Arabidopsis thaliana* phytoalexin camalexin and its role in

- Arabidopsis*–pathogen interactions. *Mol. Plant–Microbe Interact.* **9**, 748–757.
- Schoonbeek, H., Del Sorbo, G. and De Waard, M.A. (2001) The ABC transporter BcatrB affects the sensitivity of *Botrytis cinerea* to the phytoalexin resveratrol and the fungicide fenpiclonil. *Mol. Plant–Microbe Interact.* **14**, 562–571.
- Sellam, A., Iacomi-Vasilescu, B., Hudhomme, P. and Simoneau, P. (2006a) In vitro antifungal activity of brassinin, camalexin and two isothiocyanates against the crucifer pathogens *Alternaria brassicicola* and *Alternaria brassicae*. *Plant Pathol.*, in press.
- Sellam, A., Poupard, P. and Simoneau, P. (2006b) Molecular cloning of *AbGst1* encoding a glutathione transferase differentially expressed during exposure of *Alternaria brassicicola* to isothiocyanates. *FEMS Microbiol. Lett.* **258**, 241–249.
- Sharma, K.G., Mason, D.L., Liu, G., Rea, P.A., Bachhawat, A.K. and Michaelis, S. (2002) Localization, regulation, and substrate transport properties of Bpt1p, a *Saccharomyces cerevisiae* MRP-type ABC transporter. *Eukaryot. Cell*, **1**, 391–400.
- Smith, S.J., Crowley, J.H. and Parks, L.W. (1996) Transcriptional regulation by ergosterol in the yeast *Saccharomyces cerevisiae*. *Mol. Cell Biol.* **16**, 5427–5432.
- Thomma, B.P., Nelissen, I., Eggermont, K. and Broekaert, W.F. (1999) Deficiency in phytoalexin production causes enhanced susceptibility of *Arabidopsis thaliana* to the fungus *Alternaria brassicicola*. *Plant J.* **19**, 163–171.
- Tierens, K.F., Thomma, B.P., Brouwer, M., Schmidt, J., Kistner, K., Porzel, A., Mauch-Mani, B., Cammue, B.P. and Broekaert, W.F. (2001) Study of the role of antimicrobial glucosinolate-derived isothiocyanates in resistance of *Arabidopsis* to microbial pathogens. *Plant Physiol.* **125**, 1688–1699.
- Urban, M., Bhargava, T. and Hamer, J.E. (1999) An ATP-driven efflux pump is a novel pathogenicity factor in rice blast disease. *EMBO J.* **18**, 512–521.
- Van Etten, H.D., Mansfield, J.W., Bailey, J.A. and Farmer, E.E. (1994) Two classes of plant antibiotics: phytoalexins versus 'phytoanticipins'. *Plant Cell*, **6**, 1191–1192.
- Veen, M. and Lang, C. (2005) Interactions of the ergosterol biosynthetic pathway with other lipid pathways. *Biochem. Soc. Trans.* **33**, 1178–1181.
- Wang, Y. and Casadevall, A. (1994) Growth of *Cryptococcus neoformans* in presence of L-DOPA decreases its susceptibility to amphotericin B. *Antimicrob. Agents Chemother.* **38**, 2648–2650.
- Winer, J., Jung, C.K., Shackel, I. and Williams, P.M. (1999) Development and validation of real-time quantitative reverse transcriptase-polymerase chain reaction for monitoring gene expression in cardiac myocytes *in vitro*. *Anal. Biochem.* **270**, 41–49.
- Zakrzewska, A., Palamarczyk, G., Krotkiewski, H., Zdebska, E., Saloheimo, M., Penttila, M. and Kruszewska, J.S. (2003) Overexpression of the gene encoding GTP: mannose-1-phosphate guanyltransferase, mpg1, increases cellular GDP-mannose levels and protein mannosylation in *Trichoderma reesei*. *Appl. Environ. Microbiol.* **69**, 4383–4389.
- Zhao, J., Chen, Y.H. and Kwan, H.S. (2000) Molecular cloning, characterization, and differential expression of a glucoamylase gene from the basidiomycetous fungus *Lentinula edodes*. *Appl. Environ. Microbiol.* **66**, 2531–2535.

SUPPLEMENTARY MATERIAL

The following supplementary material is available for this article:

Table S1 Expression levels of sequences randomly selected from the AI-ITC cDNA library in *Alternaria brassicicola* exposed to AI-ITC and Bz-ITC. Numerical data.

Table S2 Expression levels of sequences randomly selected from the camalexin cDNA library in *Alternaria brassicicola* exposed to camalexin. Numerical data.

Table S3 Expression levels of sequences selected from the AI-ITC and camalexin cDNA libraries during the interaction between *Alternaria brassicicola* and *Arabidopsis thaliana*. Numerical data.

Table S4 Expression levels of sequences selected from the AI-ITC and camalexin cDNA libraries during the interaction between *Alternaria brassicicola* and *Raphanus sativus*. Numerical data.

This material is available as part of the online article from: <http://www.blackwell-synergy.com/doi/full/10.1111/j.1365-2745.2007.00387.x>

Please note: Blackwell Publishing is not responsible for the content or functionality of any supplementary materials supplied by the authors. Any queries (other than missing material) should be directed to the corresponding author for the article.